

# WonderVerse: Extendable 3D Scene Generation with Video Generative Models

Hao Feng<sup>1\*</sup> Zhi Zuo<sup>2\*</sup> Jia-Hui Pan<sup>3</sup> Ka-Hei Hui<sup>3</sup> Yihua Shao<sup>4</sup> Qi Dou<sup>3</sup>  
Wei Xie<sup>1†</sup> Zhengzhe Liu<sup>5†</sup>

<sup>1</sup>Central China Normal University <sup>2</sup>Nanjing University of Aeronautics and Astronautics

<sup>3</sup>The Chinese University of Hong Kong <sup>4</sup>University of Science and Technology Beijing

<sup>5</sup>Lingnan University

## Abstract

We introduce WonderVerse, a simple but effective framework for generating extendable 3D scenes. Unlike existing methods that rely on iterative depth estimation and image inpainting, often leading to geometric distortions and inconsistencies, WonderVerse leverages the powerful world-level priors embedded within video generative foundation models to create highly immersive and geometrically coherent 3D environments. Furthermore, we propose a new technique for controllable 3D scene extension to substantially increase the scale of the generated environments. Besides, we introduce a novel abnormal sequence detection module that utilizes camera trajectory to address geometric inconsistency in the generated videos. Finally, WonderVerse is compatible with various 3D reconstruction methods, allowing both efficient and high-quality generation. Extensive experiments on 3D scene generation demonstrate that our WonderVerse, with an elegant and simple pipeline, delivers extendable and highly-realistic 3D scenes, markedly outperforming existing works that rely on more complex architectures.

## 1. Introduction

3D scene generation is a fundamental task in the vision community due to its wide-ranging applications in Virtual Reality, Mixed Reality (VR/MR), robotics, self-driving vehicles, and more. However, creating extendable and large-scale 3D scenes poses significant challenges. First, there is a lack of large-scale, high-quality datasets of 3D scenes. Second, generating realistic and geometrically accurate 3D scenes is inherently complex due to the unstructured nature of 3D space and the need to capture intricate object relationships and environmental context. Third, seamlessly extending 3D scenes while maintaining consistency and coherence

remains a significant challenge.

To generate extendable 3D scenes, recent studies [9, 14, 20, 55, 56] leverage 2D generative models for 3D scene generation. These methods typically iteratively extend a given image to synthesize views from new camera poses. Typically, they first estimate a depth map from the input image, project it into 3D, and then use an image inpainting model to extend the scene from novel viewpoints. This iterative process builds and extends the 3D environment. However, the quality of scenes generated by these approaches remains limited. As shown in Figure 4, a primary issue is geometric distortion, arising from the scale ambiguity of single-view depth estimation and the lack of consistent camera parameters across iterations. Additionally, error accumulation is a concern due to the iterative application of depth estimation and inpainting during scene expansion. Furthermore, seams and discontinuities can appear between regions generated in different iterations. Overall, the iterative discrete-view-based generation pipeline inherently results in unsatisfactory scene quality.

Going beyond existing works that rely on image generation technics, we propose a simple yet effective approach to leverage the recent advancements of video generative models [7, 23, 42, 53, 58, 61] to produce highly immersive and superior-quality 3D scenes. Our approach is motivated by an intuitive but thought-provoking fact that a video with a circular camera trajectory can naturally represent a 3D scene with good view consistency. This implies that the video, compared with images, has a smaller domain gap with 3D representations. In addition, we can fully utilize the rich prior knowledge of video generative models for 3D scene generation without requiring any 3D scene dataset. More importantly, the generation process does not require iteratively generating discrete view of images in previous methods; thus, unlike existing works, our approach is inherently free from issues like scale ambiguity of depth, camera parameter inconsistency, and error accumulation throughout iterative generation.

To achieve this, a natural initial thought is to combine

\*Equal contribution.

†Corresponding author.

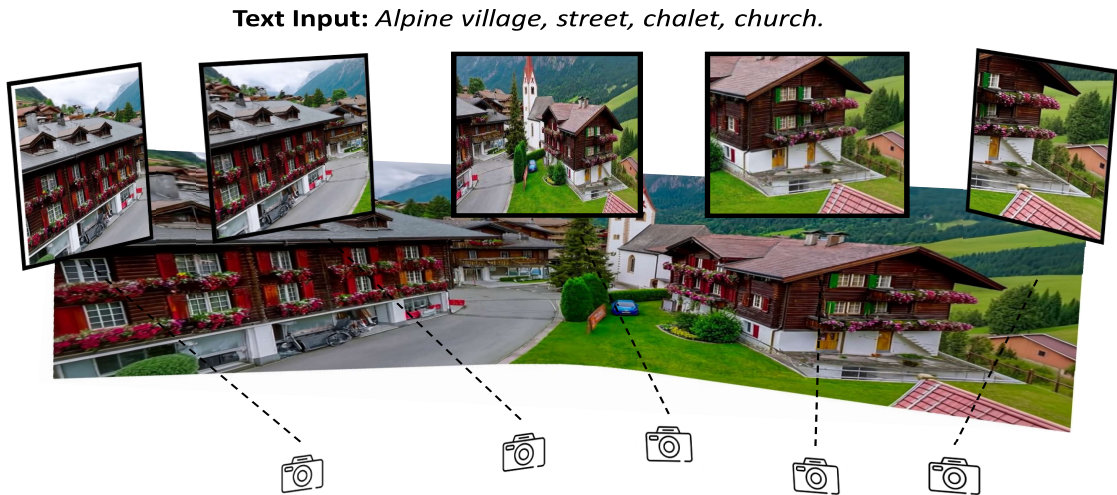


Figure 1. WonderVerse is able to create large-scale, coherent, extendable, and high-quality 3D scenes from a text.

video generative models with 3DGS (3D Gaussian Splatting) [22] for 3D scene generation. Nevertheless, this simple combination does not yield satisfactory results and cannot enable extendable 3D scene generation. Firstly, the scale of the generated scene is restricted by the capabilities of the video generative model itself. Moreover, as recent works [6, 33] have shown, generated videos can suffer from geometric inconsistencies across different frames. These inconsistencies result in substantial distortions in the resulting 3D scenes.

To address these issues, we present WonderVerse, a simple but effective extendable 3D scene generative model powered by video generative models. After generating a circular video sequence from the text input, we present a new 3D scene extension approach by extending the video at different views to form multiple extended videos, enabling large-scale 3D scene generation. Besides, we find COLMAP camera pose estimation effectively flags the geometric issue: inconsistent videos produce erratic camera poses and discontinuous trajectory. Based on the observation, we introduce an abnormal sequence detection module that evaluates the continuity of the estimated camera trajectory to enhance geometric coherence. With the consistent and coherent video sequences, we reconstruct the 3D scene. Note that our approach is compatible to various 3D reconstruction approaches for both efficient (DUST3R [43]) and high-quality (3DGS [22]) 3D scene generation.

As illustrated in Figure 1, our WonderVerse can create an extendable and highly immersive 3D scene from a piece of text. Furthermore, both qualitative and quantitative experimental results demonstrate that WonderVerse’s

neat and simple pipeline leads to state-of-the-art extendable and highly-realistic extendable 3D scene generation. Our approach demonstrates that sophisticated results can be attained through our highly elegant design. **Codes will be released upon publication.**

In summary, the key contributions of WonderVerse are:

- We propose a simple yet effective approach to leverage video generative models for the extendable 3D scene generation task, surpassing image-based iterative pipelines.
- We introduce a new video-driven 3D scene extension approach to scale up the generated environments.
- We develop an abnormal sequence detection module to enhance the geometric consistency of both generated videos and 3D scenes.
- WonderVerse achieves state-of-the-art extendable and highly-realistic 3D scene generation through a surprisingly neat and simple pipeline, significantly outperforming existing methods with far more complex architectures.

## 2. Related Works

In this section, we will briefly introduce the development of novel view synthesis (NVS), video generation for 3D reconstruction, and extendable 3D scene generation.

### 2.1. Novel View Synthesis

Novel view synthesis (NVS) is a fundamental vision task to produce a 3D scene from multi-view input images, allowing the rendering of images from novel views. Some traditional methods tackle the problem by formulating 3D scenes as light fields [10, 24], multi-view depth images [16], or blend-

ing of a collection of input images [40]. Rather than relying on handcrafted heuristics for constructing 3D scenes, the community later adopts deep learning techniques for NVS [18, 31]. Among these approaches, NeRF [31] has achieved success in improving the image’s quality, resulting in an explosion of follow-up methods [2, 4, 30, 35, 59? ] Afterwards, 3D Gaussian Splatting (3DGS) [22] is introduced as a 3D representation that enables fast training and real-time rendering while maintaining high-quality reconstruction results. This has motivated a series of follow-up works [11, 21, 57] that aim to further improve the quality and efficiency of the 3DGS representation. Recently, instead of employing an expensive optimization process, DUST3R [43] innovatively introduces a pointmap representation, enabling end-to-end 3D reconstruction with fast speed and promising performance. In this work, we demonstrate that our approach is compatible to different 3D reconstruction methods, such as 3DGS and DUST3R.

## 2.2. Image and Video Generative Models for MVS and 3D Reconstruction

Recent progress in foundation models for image [34] and video [?] generation has driven the exploration of their use in 3D reconstruction. Image generative models can be fine-tuned with multi-view data for novel-view synthesis and 3D reconstruction of objects [27, 29] and scenes [15, 48]. This strategy has been extended to video foundation models, enabling video generation with controlled camera motion for 3D reconstruction [1, 17, 25, 41, 42, 44, 52]. Nevertheless, these methods primarily target object-level or limited-scale reconstruction and cannot directly adapt to our extendable 3D scene generation task. Our objective is to generate extendable 3D scenes, requiring models with the imaginative ability to extend 3D scenes beyond the initial input.

## 2.3. Extendable 3D Scene Generation

Another branch of works explore extendable 3D scene generation. Existing works like [12, 26, 50, 51, 60] only focus on urban environments and cannot be generalized to other scenes, restricting their semantic scope. For unbounded nature scenes, methods like [5, 8] requires multi-view data, while others [28, 45, 49] rely on 3D scene datasets. To avoid such data dependencies, Text2Room [20], SceneScape [14], LucidDreamer [9], WonderJourney [56], WonderWorld [55] generate scenes iteratively with depth estimation and inpainting. Among existing approaches, **these methods are the most relevant ones to our work.** However, their iterative pipelines inherently suffers from geometric distortion, discontinuity, and error accumulation during scene expansion, ultimately hampering scene quality and motivating our WonderVerse framework. In this work, we seek to overcome the above challenges and leverage video generative models to generate more immersive and expandable scenes.

## 3. Methods

In this section, we will introduce our *WonderVerse* which is illustrated in Figure 2. Given a text description, the WonderVerse first generates a video that continuously presents the scene circularly. It then extends the scene by creating videos guided by the left and right views. Additionally, the framework estimates the camera pose sequence based on the generated videos and detects abnormal sequences by identifying discontinuities in camera movements. The frames corresponding to these abnormal sequences will be regenerated until all pass the filtering criteria. Finally, a 3D scene reconstruction is performed to construct the complete scene.

### 3.1. Video Generation and Extension

Most existing works on extendable 3D scene generation relies on iterative image generation. Such a design can hinder the quality of the generated results due to the significant domain gap between images and 3D representations. Simply stitching multiple images together to construct a scene often leads to geometric inconsistencies. Inspired by the rapid development of video generative models like [23], we reconsider the problem by leveraging superior generative capability of such models. Therefore, we propose to address the extendable 3D scene generation task through the lens of video generation.

Given Text Prompt  $P$ , we perform text-guided video generation [23] to obtain high-quality initial video  $V_{init} \in \mathbb{R}^{T \times H \times W \times 3}$ , where  $H$  and  $W$  denotes the height and weight of each frames, respectively.  $T$  denotes the length of the video. 3 denotes RGB channels. To enrich the scene, we further perform video-based scene extensions by extending the initial video. To maintain style consistency, we use the first frame  $V_{init}^{t=1}$  and last frame  $V_{init}^{t=T}$  of the initial video as references and generate two new videos from left and right, respectively:  $V_{extend}^{left} \in \mathbb{R}^{T' \times H \times W \times 3}$  and  $V_{extend}^{right} \in \mathbb{R}^{T' \times H \times W \times 3}$  with prompts different from the initial input,  $V_{init}$ . Then, we combine them into an extended video  $\{V_{extend}^{left}, V_{init}, V_{extend}^{right}\}$  with length  $T + 2T'$ . The video extension can be applied repeatedly  $n$  times, taking  $V_{input}$  as the initial video for the next iteration, further enriching the scene and yielding  $V_{input} = \{V_{extend}^{left_n}, V_{extend}^{left_{n-1}}, \dots, V_{init}, \dots, V_{extend}^{right_{n-1}}, V_{extend}^{right_n}\} = \{V_1, V_2, \dots, V_{2n+1}\}$ . Figure 2 (a) illustrates two iterations of video extension. More details can be found in Sec. 4.

### 3.2. Camera Parameters Estimation

Previous works [9, 20, 55, 56] extend images to 3D scenes through iterative image generation, camera parameter estimation, and rendering. However, their camera trajectories are often subjectively defined, leading to potential angle mismatches between rendered and synthesized images. This results in diminished scene quality and visual incon-

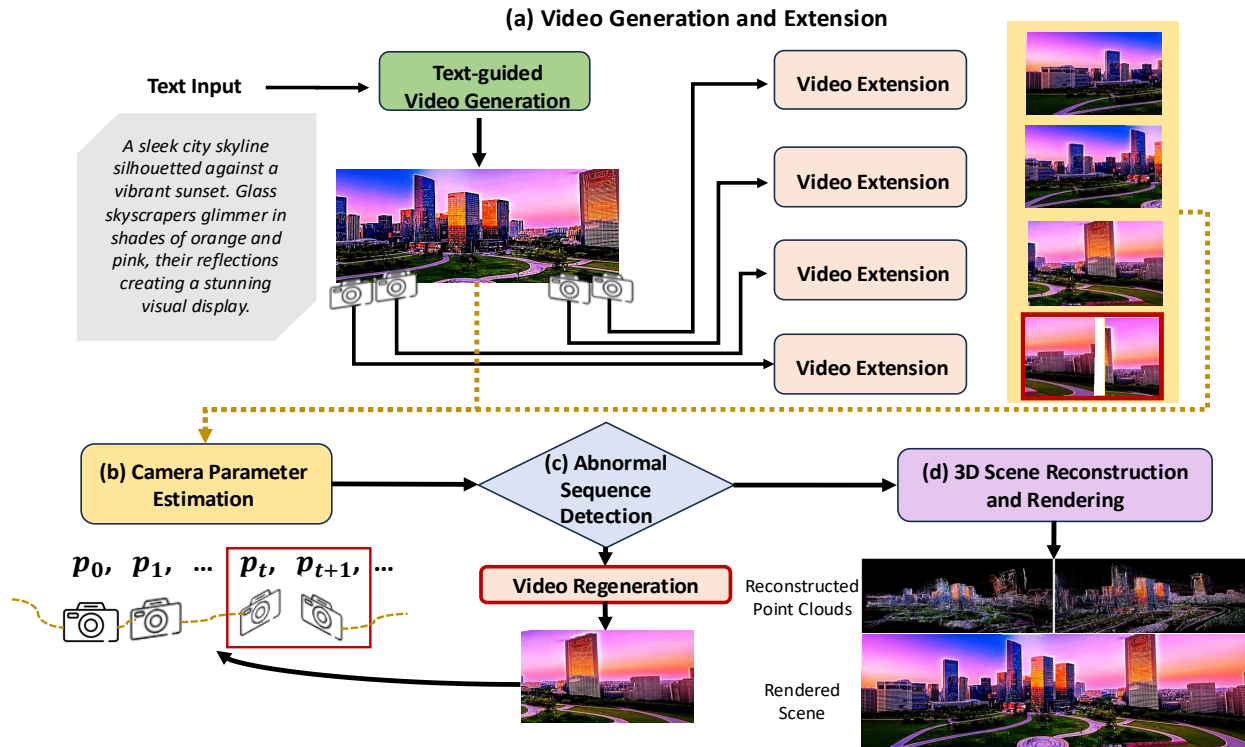


Figure 2. **Illustration of our WonderVerse.** This framework includes: (a) a text-guided video generation and extension module that produces a video of a scene circularly in a continuous shot, followed by extensions to both sides; (b) a camera parameter estimation module that predicts the camera pose sequence; (c) an abnormal sequence detection module that identifies discontinuous camera poses and regenerates the corresponding videos; and (d) a 3D scene reconstruction and rendering module to construct the generated scene.

sistencies. In contrast, leveraging the inherent continuity of video, our approach uses COLMAP [38, 39] to compute consistent camera parameters for 3D scene optimization, thus achieving enhanced geometric consistency in the generated 3D scenes.

To acquire point clouds and camera poses, we utilize COLMAP, a Structure from Motion (SfM) and Multi-View Stereo (MVS) pipeline that yields accurate results for 3D scene initialization. For video data, we employ sequential matching as our feature-matching strategy within SfM to reduce computational complexity and accelerate estimation. Furthermore, to enhance matching quality, we apply guided matching, which leverages known geometric information to direct feature matching and constrain the search space.

### 3.3. Abnormal Sequence Detection

Although the video generation model is powerful, not all videos generated from prompts are suitable for scene generation. A common issue degrading 3D scene generation is the geometric inconsistency of video generative models [6, 33]. We observed that geometric inconsistencies are effectively revealed by erratic camera pose estimations from COLMAP. Assuming smooth video genera-

tion implies smooth camera motion, geometric inconsistencies disrupt pose estimation, resulting in random, inaccurate poses. We empirically found a strong correlation between visually identified geometric inconsistency and unreliable COLMAP poses across a dataset with 320 videos, indicating pose estimation as a practical indicator.

Based on the above observation, we design an abnormal sequence detection scheme that identifies these videos by locating discontinuities in the camera pose trajectory. We identify discontinuities by monitoring changes in camera position and rotation. A sequence is flagged as discontinuous and geometrically inconsistent if position shifts exceed 5 units or rotation changes exceed 0.5 degrees. If any abnormal sequences are detected, the corresponding videos undergo a re-generation scheme in which the video extension or generation, and the camera parameter estimation are performed again until all sequences pass the criteria.

Using the input videos and extracted camera poses (denoted by rotation  $R$  and position  $P$  for each frame), our algorithm iteratively evaluates the continuity of camera movements across video frames. In each iteration, the difference in camera poses between consecutive frames is computed. Should this difference surpass a defined threshold, the cor-



---

**Algorithm 1:** Abnormal sequence detection.

---

```
1 Inputs: video length  $l_{\text{video}}$ ,
2 input videos  $V_{\text{input}} = \{V_1, V_2, \dots, V_j, \dots, V_{2n+1}\}$ ,
3 video re-generation function  $\Psi(\cdot)$ ,
4 camera extrinsic parameters list
5  $L = \{(R_1, P_1), (R_2, P_2), \dots, (R_l, P_l), \dots\}$ ,
6 camera parameter estimation function  $\Gamma(\cdot)$ ,
7 extrinsic parameter threshold  $\theta = \{\theta_R, \theta_P\}$ 
8 Outputs: stable scene video
    $V_{\text{output}} = \{\tilde{V}_1, \tilde{V}_2, \dots, \tilde{V}_j, \dots, \tilde{V}_{2n+1}\}$ 
9 Initialization: sort  $L$  by timestamp
10  $l \leftarrow 2$ ;  $V_{\text{output}} \leftarrow V_{\text{input}}$ 
11 while  $l < |L|$  do
12    $\Delta R_l, \Delta P_l \leftarrow \text{Abs}(R_l - R_{l+1}), \text{Abs}(P_l - P_{l+1})$ 
13   if  $\Delta R_l > \theta_R$  or  $\Delta P_l > \theta_P$  then
14      $j \leftarrow \text{GetCurrentVideoID}(l)$ 
15      $\tilde{V}_j \leftarrow \Psi(V_j)$   $\triangleright$  re-generate unstable segment
16      $V_{\text{output}} \leftarrow \text{Update}(V_{\text{output}}, \tilde{V}_j)$ 
17      $L \leftarrow \text{Update}(L, \Gamma(\tilde{V}_j))$ 
18      $\triangleright$  Re-estimate the camera parameters
19      $l \leftarrow \text{GetStartFrameID}(\tilde{V}_j)$ 
20      $\triangleright$  Back to the start of  $\tilde{V}_j$ 
21   else
22      $l \leftarrow l + 1$ 
23   end
24 end
25 return  $V_{\text{output}}$ 
```

---

responding segment is marked for replacement, and camera parameters are re-estimated to ensure consistency. Conversely, if the difference remains within the threshold, the segment is deemed satisfactory, and the algorithm proceeds to the next frame. This iterative evaluation across all segments, allowing for the identification and correction of any anomalies in the video sequence.

### 3.4. 3D Scene Reconstruction and Rendering

To obtain an immersive and high-quality scene, we employ an advanced 3D representations method, i.e. 3DGS [22], which supports real-time rendering and is faster in training.

Let us define a 3D Gaussian  $i$  that is parameterized by a centroid  $\mu_i$ , a covariance matrix  $\Sigma_i$ , opacity  $\sigma_i$  and color  $c_i$ , representing the first three degrees of the spherical harmonic (SH) coefficients. These properties are learnable and optimized during training. In practice, the covariance matrix is decomposed into a scaling matrix  $S_i$  and a rotation matrix  $R_i$  to ensure that the covariance matrix remains positive semi-definite and retains physical meaning, i.e.  $\Sigma_i = R_i S_i S_i^T R_i^T$ . To project 3D onto 2D, the covariance matrix is approximated by the Jacobian matrix and the

world-to-camera matrix:  $\Sigma'_i = JW\Sigma_iW^TJ^T$ . Then, the opacity of Gaussian at image plane  $p'_i$  is computed as follows:

$$\alpha'_i = \sigma_i \cdot \exp\left(-\frac{1}{2}(p'_i - \mu'_i)^T(\Sigma'_i)^{-1}(p'_i - \mu'_i)\right). \quad (1)$$

Finally, the color  $C$  of pixel  $p$  is:

$$C(p) = \sum_{i \in N} c_i \cdot \alpha'_i \prod_{j=1}^{i-1} (1 - \alpha'_j). \quad (2)$$

After abnormal sequence detection, we derive a set of valid camera parameters, i.e.  $L = \{(R_1, P_1), (R_2, P_2), \dots\}$ , where  $R, P$  denotes rotation and position respectively. Then we render  $I_{ren}$  with 3DGS from each camera view, and it corresponds to a frame  $I_{gt}$  of the generated video. Then we compute  $\mathcal{L}_1$  loss and  $\mathcal{L}_{D-SSIM}$  loss between  $I_{ren}$  and  $I_{gt}$ . Finally, our loss function is:

$$\mathcal{L} = (1 - \lambda)\mathcal{L}_1 + \lambda\mathcal{L}_{D-SSIM}. \quad (3)$$

where  $\mathcal{L}_{D-SSIM}$  is the SSIM loss that optimizes the image quality, and  $\mathcal{L}_1$  is the L1 loss,  $\lambda$  is set as 0.2.

In contrast to prior works that rely on point clouds [9, 20, 56] or less common data formats such as layered images [55] as intermediate representations, WonderVerse directly generates images and corresponding camera poses. This design significantly enhances compatibility, allowing us to leverage well-established 3D reconstruction methods that natively accept image and pose inputs, such as the recent DUS3R [43]. This streamlined approach enables efficient 3D scene generation, with the potential for further improvements as reconstruction techniques advance.

## 4. Experiments

In this section, first, we will introduce the implementation details and evaluation metrics. Then we show our generative results and also compare with existing works both quantitatively and qualitatively. Subsequently, we conduct ablation study on our key modules. Note that we provide additional generative results in the supplementary materiel.

### 4.1. Experimental Settings

**Implementation Details** Starting with a text prompt, WonderVerse first generates an initial circular video. The first and last frames of this video serve as seeds for scene extension. To extend the scene, these seed frames are incorporated into the video generative model with text prompts, guiding the generation of additional videos that seamlessly extend the existing scene. This extension process is iterative and can be repeated for virtually infinite scene growth. In our experiments, we performed four extension iterations, adding two videos to the left and two to the right of the



(a) A bright kitchen with white cabinets, stainless steel appliances, and a central island, accented by a wooden dining table.



(b) A quiet workshop filled with tools neatly hung on the walls, a sturdy workbench ready for projects, and shelves stocked with materials, all waiting for creative inspiration.



(c) The playground in a residential area, with abundant street trees, cars parked on the road, and single-family homes.



(d) A charming town square surrounded by quaint, colorful buildings with wrought-iron balconies; a cobblestone path leads to a central fountain, its water still and reflecting the blue sky, while flower boxes add bursts of color to the scene.

Figure 3. WonderVerse generates large-scale, extendable, coherent, and high-fidelity 3D scenes, both indoors and outdoors. Dashed lines show the camera’s direction during scene extension.

original scene. Our text prompts follow a template: “aerial shot, soft lighting, around left [or right], realistic, high-quality, displaying [scene description]”. Camera motion control was facilitated via the API provided by the video generative models. For initial scene generation, we utilized the Hunyuan video model [23]. However, as image-conditioned video generation was not yet available for Hunyuan at the time, we adopted Gen-3 Alpha [36] for the subsequent scene extension steps.

In our experiments, we generate an initial scene for each test example and extend it by creating four additional scenes, yielding five scenes per example and twenty in total. In contrast to WonderWorld’s image-based scenes, each extension in our approach produces a complete video scene. This video representation offers a significant advantage in immersiveness and richness over static image scenes of existing works.

**Evaluation metrics** Following recent work [55], we evaluate our scenes using CLIP-Score (CLIP-S) [19], Q-Align [47], and NIQE [32]. CLIP-S measures text-image alignment by comparing CLIP feature embeddings. Q-Align, trained with human scoring patterns and instruction tuning, assesses quality, correlating well with subjective human judgments. NIQE, a no-reference image quality metric, evaluates quality degradation by comparing spatial features to a pristine natural image model.

## 4.2. Our Results of Extendable 3D Scenes

In Figure 3, we present compelling examples of extendable indoor and outdoor 3D scenes generated by WonderVerse

across. Figure 3 (a, b) illustrate the remarkable realism and rich detail achieved in our indoor scenes, with flawless geometric integrity. Also, the scenes are faithful and immersive visualizations of the described environments. For example, in (b) we generate a workshop, with “tools hanging on the wall”, a “sturdy workbench”, and “shelves stocked with materials”. All the objects are rendered with photorealistic quality and placed within a geometrically coherent space. Figure 3 (c, d) further exemplifies this capability in outdoor scenarios. For example, in (c), a playground in a residential area is generated, where all textually described components like “car” and “tree” are seamlessly integrated with remarkable visual fidelity. Also, our scenes have great geometric consistency and no obvious mistakes or breaks that look unnatural. This shows the strength of WonderVerse in making highly immersive and extendable 3D scenes. Please refer to the supplementary material for additional generative results across diverse scenes and styles of WonderVerse. Besides, we also demonstrate users can generate extendable 3D scenes iteratively using WonderVerse.

## 4.3. Comparison with Existing Works

**Baseline Approaches** We compare our WonderVerse with recent works WonderWorld [55] and LucidDreamer [9] both qualitatively and quantitatively. Since these two baselines need an image as input while our method only needs a text prompt as input, for fair comparison, we take a random frame of our generated video and feed it into their models for 3D scene generation. Note that WonderWorld [55]’s layered image representation, including a sky layer, makes



Figure 4. Qualitative comparison with existing works.

it less suited for indoor scene generation. Consequently, our primary comparative analysis focuses on outdoor scenes.

**Qualitative Comparison** Figure 4 visually demonstrates WonderVerse’s clear superiority over existing methods. As shown in Fig 4 (a), LucidDreamer’s generated scene is far from satisfactory, blurry, obscured by an odd frame-like artifacts, and lacking in detail. WonderWorld (Figure 4 (b)), while generating a broader view, suffers from geometric discontinuities, as indicated by the visibly stitched and unnatural scene. In contrast, WonderVerse (Figure 4 (c)) produces a satisfactory and geometrically sound 3D scene. The shot of the university buildings is rendered with 3DGS [22] with high fidelity, sharp textures, coherent architecture, and natural sky and lighting. The geometric integrity is maintained seamlessly across the scene, addressing the limitations apparent in both LucidDreamer’s quality and WonderWorld’s geometric consistency. Please refer to the supplementary material for additional comparison results with existing works, including Text2room [20].

**Quantitative Comparison.** We quantitatively compare WonderVerse to prior work LucidDreamer [9] and WonderWorld [55], with results shown in Table 1 for both outdoor and indoor scenes. Our method demonstrates state-of-the-art scene generation, outperforming existing methods in semantic alignment, structural consistency, and perceptual quality. Notably, for outdoor scenes, WonderVerse achieves the best CLIP-S score (0.9219), indicating superior semantic alignment, along with SOTA Q-align and NIQE scores, demonstrating high generation quality. Similarly, for indoor scenes, WonderVerse significantly surpasses LucidDreamer across all metrics, achieving a new SOTA CLIP-S score of 0.9639, again affirming excellent text-scene semantic alignment and high-quality 3D indoor scene generation. Note that WonderWorld cannot generate indoor scene due to its sky layer, so we do not compare with approach in the indoor setting.

#### 4.4. Ablation Studies

In this section, we examine the key modules of our approach, including abnormal sequence detection and scene extension. We also compare different 3D representation methods 3DGS [22] and DUS3R [43] to demonstrate the compatibility of our approach.

Table 1. Evaluation on novel view renderings.

Scene Type	Method	CLIP-S ( $\uparrow$ )	Q-align ( $\uparrow$ )	NIQE ( $\uparrow$ )
Outdoor	LucidDreamer [9]	0.4200	2.6704	0.7786
	WonderWorld [55]	0.7817	2.8302	0.7127
	WonderVerse (ours)	<b>0.9219</b>	<b>3.2229</b>	<b>0.7806</b>
Indoor	LucidDreamer [9]	0.4633	3.9870	0.6655
	WonderVerse (ours)	<b>0.9639</b>	<b>4.2680</b>	<b>0.7119</b>

Table 2. Evaluation metrics of abnormal sequence detection.

	Q-align	NIQE
W/o abnormal sequence detection	0.67	3.39
W abnormal sequence detection	<b>0.75</b>	<b>3.64</b>

#### 4.4.1. Abnormal Sequence Detection

In this section, we study the effectiveness of our abnormal sequence detection. As illustrated in Figure 5, we present the generated 3D scene with and without abnormal sequence detection. Without our detection algorithm, noticeable artifacts degrade the generated 3D scene due to the geometric inconsistency of the generated video. In contrast, when abnormal sequences are detected and addressed, the generative quality is much higher. The improvement is further demonstrated by quantitative evaluations in Table 2. The results of both the Q-Align and NIQE metrics clearly show the significant improvements of our abnormal sequence detection module, demonstrating that this design effectively enhances the quality of the generated 3D scenes.

#### 4.4.2. Scene Extension

Figure 6 visually demonstrates how our scene extension strategy effectively increases the scale and scope of generated 3D scenes. We compare scenes generated with and without our extension technique. Figure 6 (a) shows the limited scope of the scene without extension; these images show a restricted view of the living room, focusing on a sofa section and the fireplace. In contrast, Figure 6 (b,c) vividly illustrates the expanded scene. The view is now significantly wider, revealing a larger portion of the living room, including more of the L-shaped sofa, extended window areas, and a broader view of the floor. These visuals confirm that our scene extension not only increases the scene’s scale but also successfully maintains both geometric and stylistic





Figure 5. Generated 3D scene without and with our abnormal sequence detection module.

(a) Video before scene extension (b) Video after scene extension



(c) The final generated scene after extension.

Figure 6. Video results of a generated 3D scene. Starting from (a), we extended the video to (b) with high quality and maintained good geometric consistency, resulting in a realistic extended scene (c). For the best experience of GIF animations (a, b), please view them in Acrobat or similar PDF readers.

consistency, as evidenced by the consistent style and geometry of the furniture and room elements across the expanded view. The extended scene is richer in details and provides a more comprehensive and immersive representation of the environment compared to the limited initial scenes.

#### 4.4.3. Efficient vs. High-quality

Our method is highly flexible and can support a wide variety of 3D representation method, such as 3DGS [22] and DUST3R [43]. In this section, we replace 3DGS and its associated components in our pipeline with DUST3R to demonstrate the adaptability of our approach. Experimental results reveal that DUST3R enables efficient generation, achieving speeds over 10× faster than 3DGS. Conversely, high-quality generation can be achieved with 3DGS, as shown in Figure 7.



(a) Efficient DUST3R (b) High-quality 3DGS

Figure 7. Generated 3D scene with different 3D reconstruction methods. (a) efficient reconstruction by DUST3R; (b) High-quality generation by 3DGS. (b) is a GIF animation, viewable in PDF readers like Acrobat.

## 5. Conclusion and Limitation

In this paper, we introduced WonderVerse, a framework that offers a surprisingly simple yet remarkably effective approach to generating extendable 3D scenes. Moving beyond the complexities of iterative depth estimation and image inpainting common in prior works, WonderVerse leverages the inherent world-level priors of video generative foundation models to achieve highly immersive and geometrically consistent 3D environments. Our contributions extend beyond the initial scene generation with a new technique for controllable scene expansion, enabling substantial scaling of generated environments, and an innovative abnormal sequence detection module that utilizes camera trajectory to effectively address geometric inconsistencies. As demonstrated through extensive experiments, WonderVerse can generate extendable and highly realistic 3D scenes with an elegant and streamlined pipeline, markedly outperforming existing works with more complex architectures.

Our WonderVerse framework, while effective, has certain limitations. First, The quality of our simulated 3D environments is inherently limited by existing video generation models. Second, our model mainly focuses on static 3D scene generation due to the use of 3DGS and DUST3R



for reconstruction. To overcome this, an exciting avenue for future research is combine with recent advancements in dynamic scene representation [13, 46, 54] to pave the way for generating dynamic and animated 3D environments.

## References

- [1] Omer Bar-Tal, Hila Chefer, Omer Tov, Charles Herrmann, Roni Paiss, Shiran Zada, Ariel Ephrat, Junhwa Hur, Guanghui Liu, Amit Raj, et al. Lumiere: A space-time diffusion model for video generation. In *SIGGRAPH Asia 2024 Conference Papers*, pages 1–11, 2024. 3
- [2] Jonathan T Barron, Ben Mildenhall, Dor Verbin, Pratul P Srinivasan, and Peter Hedman. Mip-nerf 360: Unbounded anti-aliased neural radiance fields. In *Proceedings of the IEEE/CVF conference on computer vision and pattern recognition*, pages 5470–5479, 2022. 3
- [3] Paul J. Besl and Neil D. McKay. A method for registration of 3-d shapes. In *IEEE Transactions on Pattern Analysis and Machine Intelligence (PAMI)*, pages 239–256, 1992. 12
- [4] Wenjing Bian, Zirui Wang, Kejie Li, Jia-Wang Bian, and Victor Adrian Prisacariu. Nope-nerf: Optimising neural radiance field with no pose prior. In *Proceedings of the IEEE/CVF Conference on Computer Vision and Pattern Recognition*, pages 4160–4169, 2023. 3
- [5] Lucy Chai, Richard Tucker, Zhengqi Li, Phillip Isola, and Noah Snavely. Persistent nature: A generative model of unbounded 3d worlds. In *Proceedings of the IEEE/CVF conference on computer vision and pattern recognition*, pages 20863–20874, 2023. 3
- [6] Chirui Chang, Zhengzhe Liu, Xiaoyang Lyu, and Xiaojuan Qi. What matters in detecting ai-generated videos like sora? *arXiv preprint arXiv:2406.19568*, 2024. 2, 4
- [7] Shoufa Chen, Chongjian Ge, Yuqi Zhang, Yida Zhang, Fengda Zhu, Hao Yang, Hongxiang Hao, Hui Wu, Zhichao Lai, Yifei Hu, Ting-Che Lin, Shilong Zhang, Fu Li, Chuan Li, Xing Wang, Yanghua Peng, Peize Sun, Ping Luo, Yi Jiang, Zehuan Yuan, Bingyue Peng, and Xiaobing Liu. Goku: Flow based video generative foundation models. *arXiv preprint arXiv:2502.04896*, 2025. 1
- [8] Zhaoxi Chen, Guangcong Wang, and Ziwei Liu. Scenedreamer: Unbounded 3d scene generation from 2d image collections. *IEEE transactions on pattern analysis and machine intelligence*, 45(12):15562–15576, 2023. 3
- [9] Jaeyoung Chung, Suyoung Lee, Hyeongjin Nam, Jaerin Lee, and Kyoung Mu Lee. Luciddreamer: Domain-free generation of 3d gaussian splatting scenes, 2023. 1, 3, 5, 6, 7, 12
- [10] Michael Cohen, Steven J. Gortler, Richard Szeliski, Radek Grzeszczuk, and Rick Szeliski. The lumigraph. Association for Computing Machinery, Inc., 1996. 2
- [11] Pinxuan Dai, Jiamin Xu, Wenxiang Xie, Xinguo Liu, Huamin Wang, and Weiwei Xu. High-quality surface reconstruction using gaussian surfels. In *ACM SIGGRAPH 2024 Conference Papers*, pages 1–11, 2024. 3
- [12] Jie Deng, Wenhao Chai, Jianshu Guo, Qixuan Huang, Wenhao Hu, Jenq-Neng Hwang, and Gaoang Wang. Citygen: Infinite and controllable 3d city layout generation. *arXiv preprint arXiv:2312.01508*, 2023. 3
- [13] Yuanxing Duan, Fangyin Wei, Qiyu Dai, Yuhang He, Wenzheng Chen, and Baoquan Chen. 4d-rotor gaussian splatting: Towards efficient novel view synthesis for dynamic scenes. In *International Conference on Computer Graphics and Interactive Techniques*, 2024. 9
- [14] Rafail Fridman, Amit Abecasis, Yoni Kasten, and Tali Dekel. Scenescape: Text-driven consistent scene generation. *Advances in Neural Information Processing Systems*, 36:39897–39914, 2023. 1, 3
- [15] Ruiqi Gao, Aleksander Holynski, Philipp Henzler, Arthur Brussee, Ricardo Martin-Brualla, Pratul Srinivasan, Jonathan T Barron, and Ben Poole. Cat3d: Create anything in 3d with multi-view diffusion models. *arXiv preprint arXiv:2405.10314*, 2024. 3
- [16] Michael Goesele, Noah Snavely, Brian Curless, Hugues Hoppe, and Steven M Seitz. Multi-view stereo for community photo collections. In *2007 IEEE 11th International Conference on Computer Vision*, pages 1–8. IEEE, 2007. 2
- [17] Hao He, Yinghao Xu, Yuwei Guo, Gordon Wetzstein, Bo Dai, Hongsheng Li, and Ceyuan Yang. Cameractrl: Enabling camera control for text-to-video generation. *arXiv preprint arXiv:2404.02101*, 2024. 3
- [18] Peter Hedman, Julien Philip, True Price, Jan-Michael Frahm, George Drettakis, and Gabriel Brostow. Deep blending for free-viewpoint image-based rendering. *ACM Transactions on Graphics (ToG)*, 37(6):1–15, 2018. 3
- [19] Jack Hessel, Ari Holtzman, Maxwell Forbes, Ronan Le Bras, and Yejin Choi. CLIPScore: a reference-free evaluation metric for image captioning. In *EMNLP*, 2021. 6
- [20] Lukas Höllein, Ang Cao, Andrew Owens, Justin Johnson, and Matthias Nießner. Text2room: Extracting textured 3d meshes from 2d text-to-image models. In *Proceedings of the IEEE/CVF International Conference on Computer Vision*, pages 7909–7920, 2023. 1, 3, 5, 7, 12
- [21] Binbin Huang, Zehao Yu, Anpei Chen, Andreas Geiger, and Shenghua Gao. 2d gaussian splatting for geometrically accurate radiance fields. In *ACM SIGGRAPH 2024 conference papers*, pages 1–11, 2024. 3
- [22] Bernhard Kerbl, Georgios Kopanas, Thomas Leimkühler, and George Drettakis. 3d gaussian splatting for real-time radiance field rendering. *ACM Trans. Graph.*, 42(4):139–1, 2023. 2, 3, 5, 7, 8
- [23] Weijie Kong. Hunyuanvideo: A systematic framework for large video generative models, 2024. 1, 3, 6
- [24] Marc Levoy and Pat Hanrahan. Light field rendering. In *Seminal Graphics Papers: Pushing the Boundaries, Volume 2*, pages 441–452. 2023. 2
- [25] Haoran Li, Haolin Shi, Wenli Zhang, Wenjun Wu, Yong Liao, Lin Wang, Lik-hang Lee, and Peng Yuan Zhou. Dreamscene: 3d gaussian-based text-to-3d scene generation via formation pattern sampling. In *European Conference on Computer Vision*, pages 214–230. Springer, 2024. 3
- [26] Chieh Hubert Lin, Hsin-Ying Lee, Willi Menapace, Menglei Chai, Aliaksandr Siarohin, Ming-Hsuan Yang, and Sergey Tulyakov. Infinicity: Infinite-scale city synthesis. In *Proceedings of the IEEE/CVF international conference on computer vision*, pages 22808–22818, 2023. 3

- [27] Ruoshi Liu, Rundi Wu, Basile Van Hoorick, Pavel Tokmakov, Sergey Zakharov, and Carl Vondrick. Zero-1-to-3: Zero-shot one image to 3d object. In *Proceedings of the IEEE/CVF international conference on computer vision*, pages 9298–9309, 2023. 3
- [28] Yuheng Liu, Xinke Li, Xueting Li, Lu Qi, Chongshou Li, and Ming-Hsuan Yang. Pyramid diffusion for fine 3d large scene generation. In *European Conference on Computer Vision*, pages 71–87. Springer, 2024. 3
- [29] Xiaoxiao Long, Yuan-Chen Guo, Cheng Lin, Yuan Liu, Zhiyang Dou, Lingjie Liu, Yuexin Ma, Song-Hai Zhang, Marc Habermann, Christian Theobalt, et al. Wonder3d: Single image to 3d using cross-domain diffusion. In *CVPR*, pages 9970–9980, 2024. 3
- [30] Ricardo Martin-Brualla, Noha Radwan, Mehdi SM Sajjadi, Jonathan T Barron, Alexey Dosovitskiy, and Daniel Duckworth. Nerf in the wild: Neural radiance fields for unconstrained photo collections. In *Proceedings of the IEEE/CVF conference on computer vision and pattern recognition*, pages 7210–7219, 2021. 3
- [31] Ben Mildenhall, Pratul P Srinivasan, Matthew Tancik, Jonathan T Barron, Ravi Ramamoorthi, and Ren Ng. Nerf: Representing scenes as neural radiance fields for view synthesis. *Communications of the ACM*, 65(1):99–106, 2021. 3
- [32] Anish Mittal, Rajiv Soundararajan, and Alan C. Bovik. Making a “completely blind” image quality analyzer. *IEEE Signal Processing Letters*, 20(3):209–212, 2013. 6
- [33] Yiran Qin, Zhelun Shi, Jiwen Yu, Xijun Wang, Enshen Zhou, Lijun Li, Zhenfei Yin, Xihui Liu, Lu Sheng, Jing Shao, et al. Worldsmbench: Towards video generation models as world simulators. *arXiv preprint arXiv:2410.18072*, 2024. 2, 4
- [34] Robin Rombach, Andreas Blattmann, Dominik Lorenz, Patrick Esser, and Björn Ommer. High-resolution image synthesis with latent diffusion models. In *Proceedings of the IEEE/CVF conference on computer vision and pattern recognition*, pages 10684–10695, 2022. 3
- [35] Viktor Rudnev, Mohamed Elgharib, William Smith, Lingjie Liu, Vladislav Golyanik, and Christian Theobalt. Nerf for outdoor scene relighting. In *European Conference on Computer Vision*, pages 615–631. Springer, 2022. 3
- [36] Runway. <https://runwayml.com/research/introducing-gen-3-alpha>. 2024. 6
- [37] Radu Bogdan Rusu and Steve Cousins. 3d is here: Point cloud library (pcl). *IEEE International Conference on Robotics and Automation (ICRA)*, pages 1–4, 2011. 12
- [38] Johannes Lutz Schönberger and Jan-Michael Frahm. Structure-from-motion revisited. In *Conference on Computer Vision and Pattern Recognition (CVPR)*, 2016. 4
- [39] Johannes Lutz Schönberger, Enliang Zheng, Marc Pollefeys, and Jan-Michael Frahm. Pixelwise view selection for unstructured multi-view stereo. In *European Conference on Computer Vision (ECCV)*, 2016. 4
- [40] Noah Snavely, Steven M Seitz, and Richard Szeliski. Photo tourism: exploring photo collections in 3d. In *ACM siggraph 2006 papers*, pages 835–846. 2006. 3
- [41] Vikram Voleti, Chun-Han Yao, Mark Boss, Adam Letts, David Pankratz, Dmitry Tochilkin, Christian Laforte, Robin Rombach, and Varun Jampani. Sv3d: Novel multi-view synthesis and 3d generation from a single image using latent video diffusion. In *European Conference on Computer Vision*, pages 439–457. Springer, 2024. 3
- [42] Carl Vondrick, Hamed Pirsiavash, and Antonio Torralba. Generating videos with scene dynamics. *Advances in neural information processing systems*, 29, 2016. 1, 3
- [43] Shuzhe Wang, Vincent Leroy, Yohann Cabon, Boris Chidlovskii, and Jerome Revaud. Dust3r: Geometric 3d vision made easy. In *CVPR*, 2024. 2, 3, 5, 7, 8, 12
- [44] Zhouxia Wang, Ziyang Yuan, Xintao Wang, Yaowei Li, Tianshui Chen, Menghan Xia, Ping Luo, and Ying Shan. Motionctrl: A unified and flexible motion controller for video generation. In *ACM SIGGRAPH 2024 Conference Papers*, pages 1–11, 2024. 3
- [45] Yao Wei, Martin Renqiang Min, George Vosselman, Li Erran Li, and Michael Ying Yang. Planner3d: Llm-enhanced graph prior meets 3d indoor scene explicit regularization. *arXiv preprint arXiv:2403.12848*, 2024. 3
- [46] Guanjun Wu, Taoran Yi, Jiemin Fang, Lingxi Xie, Xiaopeng Zhang, Wei Wei, Wenyu Liu, Qi Tian, and Xinggang Wang. 4d gaussian splatting for real-time dynamic scene rendering. *2024 IEEE/CVF Conference on Computer Vision and Pattern Recognition (CVPR)*, pages 20310–20320, 2023. 9
- [47] Haoning Wu, Zicheng Zhang, Weixia Zhang, Chaofeng Chen, Chunyi Li, Liang Liao, Annan Wang, Erli Zhang, Wenxiu Sun, Qiong Yan, Xiongkuo Min, Guangtai Zhai, and Weisi Lin. Q-align: Teaching Imms for visual scoring via discrete text-defined levels. *arXiv preprint arXiv:2312.17090*, 2023. Equal Contribution by Wu, Haoning and Zhang, Zicheng. Project Lead by Wu, Haoning. Corresponding Authors: Zhai, Guangtai and Lin, Weisi. 6
- [48] Rundi Wu, Ben Mildenhall, Philipp Henzler, Keunhong Park, Ruiqi Gao, Daniel Watson, Pratul P Srinivasan, Dor Verbin, Jonathan T Barron, Ben Poole, et al. Reconfusion: 3d reconstruction with diffusion priors. In *Proceedings of the IEEE/CVF conference on computer vision and pattern recognition*, pages 21551–21561, 2024. 3
- [49] Zhennan Wu, Yang Li, Han Yan, Taizhang Shang, Weixuan Sun, Senbo Wang, Ruikai Cui, Weizhe Liu, Hiroyuki Sato, Hongdong Li, et al. Blockfusion: Expandable 3d scene generation using latent tri-plane extrapolation. *ACM Transactions on Graphics (TOG)*, 43(4):1–17, 2024. 3
- [50] Haozhe Xie, Zhaoxi Chen, Fangzhou Hong, and Ziwei Liu. Citydreamer: Compositional generative model of unbounded 3d cities. In *Proceedings of the IEEE/CVF conference on computer vision and pattern recognition*, pages 9666–9675, 2024. 3
- [51] Haozhe Xie, Zhaoxi Chen, Fangzhou Hong, and Ziwei Liu. GaussianCity: Generative gaussian splatting for unbounded 3d city generation. *arXiv preprint arXiv:2406.06526*, 2024. 3
- [52] Yiming Xie, Chun-Han Yao, Vikram Voleti, Huaizu Jiang, and Varun Jampani. Sv4d: Dynamic 3d content generation with multi-frame and multi-view consistency. *arXiv preprint arXiv:2407.17470*, 2024. 3
- [53] Zhuoyi Yang, Jiayan Teng, Wendi Zheng, Ming Ding, Shiyu Huang, Jiazheng Xu, Yuanming Yang, Wenyi Hong, Xiao-

- han Zhang, Guanyu Feng, et al. Cogvideox: Text-to-video diffusion models with an expert transformer. *arXiv preprint arXiv:2408.06072*, 2024. 1
- [54] Zeyu Yang, Hongye Yang, Zijie Pan, and Li Zhang. Real-time photorealistic dynamic scene representation and rendering with 4d gaussian splatting. In *International Conference on Learning Representations (ICLR)*, 2024. 9
- [55] Hong-Xing Yu, Haoyi Duan, Charles Herrmann, William T Freeman, and Jiajun Wu. Wonderworld: Interactive 3d scene generation from a single image. *arXiv preprint arXiv:2406.09394*, 2024. 1, 3, 5, 6, 7, 12
- [56] Hong-Xing Yu, Haoyi Duan, Junhwa Hur, Kyle Sargent, Michael Rubinstein, William T Freeman, Forrester Cole, Deqing Sun, Noah Snavely, Jiajun Wu, et al. Wonderjourney: Going from anywhere to everywhere. In *Proceedings of the IEEE/CVF Conference on Computer Vision and Pattern Recognition*, pages 6658–6667, 2024. 1, 3, 5
- [57] Zehao Yu, Torsten Sattler, and Andreas Geiger. Gaussian opacity fields: Efficient adaptive surface reconstruction in unbounded scenes. *ACM Transactions on Graphics (TOG)*, 43(6):1–13, 2024. 3
- [58] Yan Zeng, Guoqiang Wei, Jiani Zheng, Jiaxin Zou, Yang Wei, Yuchen Zhang, and Hang Li. Make pixels dance: High-dynamic video generation, 2023. 1
- [59] Kai Zhang, Gernot Riegler, Noah Snavely, and Vladlen Koltun. Nerf++: Analyzing and improving neural radiance fields. *arXiv preprint arXiv:2010.07492*, 2020. 3
- [60] Shougao Zhang, Mengqi Zhou, Yuxi Wang, Chuanchen Luo, Rongyu Wang, Yiwei Li, Zhaoxiang Zhang, and Junran Peng. Cityx: Controllable procedural content generation for unbounded 3d cities. *arXiv preprint arXiv:2407.17572*, 2024. 3
- [61] Zangwei Zheng, Xiangyu Peng, Tianji Yang, Chenhui Shen, Shenggui Li, Hongxin Liu, Yukun Zhou, Tianyi Li, and Yang You. Open-sora: Democratizing efficient video production for all. *arXiv preprint arXiv:2412.20404*, 2024. 1

# WonderVerse: Extendable 3D Scene Generation with Video Generative Models

## Supplementary Material

### 6. Additional Comparisons with Existing Works

In this section, we provide additional comparison results with LucidDreamer [9], WonderWorld [55], and Text2Room [20]. As shown in the Fig 8, 9, As visually demonstrated in Figures 8 and 9, our WonderVerse framework can generate extendable 3D scenes, achieving a significant improvement in quality, plausibility, and geometric coherence compared to existing methods.

Baseline approaches that rely on discrete image generation pipelines exhibit noticeable geometric inconsistencies. For instance, LucidDreamer produces fragmented and discontinuous 3D scenes, while Text2Room results in largely distorted 3D scenes, both exhibiting significant geometric inconsistency. WonderWorld, while improved, still exhibits discontinuities between subscenes generated iteratively, which compromises its overall visual quality and realism. On the contrary, WonderVerse produces extendable 3D scenes that are not only visually superior but also maintain geometric integrity, resulting in more believable and immersive 3D environments. This visual comparison underscores the advantage of our approach in creating extendable and coherent 3D scenes.

### 7. Additional Qualitative Results

We show additional qualitative results in Fig 11 13 15 17. We also provide the visualization of their multi-viewed point clouds as shown in Fig 10 12 14 16.

As shown in Figure 10, the reconstructed point clouds from two viewpoints capture the structural elements of an art studio, including walls, windows, and scattered objects. Figure 11 then showcases the rendered scene from multiple perspectives, effectively portraying a vibrant art studio environment populated with canvases and art supplies, consistent with the input text prompt.

Similarly, Figure 12 visualizes the 3D point cloud representing the garden’s layout, capturing the fountain and surrounding floral arrangements. Figure 13 demonstrates the rendered scene, which vividly realizes a colorful flower garden with a central fountain reflecting the sky, faithfully adhering to the descriptive text.

Besides, Figure 14 shows the point cloud reconstruction of the Taj Mahal and its surrounding environment, clearly outlining the iconic structure and pool. Figure 15 showcases the rendered scene, capturing the majestic Taj Mahal with its reflecting pool and cypress trees, demonstrating our framework’s ability to generate complex architectural scenes from textual descriptions.

Beyond generating realistic 3D scenes, our WonderVerse demonstrates the ability to create imaginative scenes that do not exist in the real world, and in diverse styles. As seen in Figure 16, the point cloud reconstruction effectively captures the intricate structure of a Lego space station, including distinct modules, astronauts, and spacecraft elements against a backdrop of stars. Figure 17 then presents the rendered scene, vividly bringing to life a futuristic Lego space station in orbit. This example, rendered in a distinct LEGO style, illustrates our framework’s capability to move beyond photorealistic scene generation. It demonstrates that WonderVerse can interpret textual descriptions to create stylized and fictional 3D environments, expanding its creative potential beyond realistic simulations.

Across these diverse examples, our method consistently generates geometrically plausible and visually compelling 3D scenes that align well with the provided text prompts.

### 8. Interactive Scene Generation

WonderVerse also enables interactive 3D scene generation. Starting with an initial video based on a text prompt, users can interactively guide scene extension by providing new text prompts to add desired objects. For example, as shown in Figure 18 (a), we interactively extended the scene by adding “**A huge fountain**” on the right side and “**A huge library**” on the left side, both successfully incorporated into the 3D scene. Compared to Figure 18 (b), where the entire scene is generated from a single initial prompt, the interactive approach in Figure 18 (a) produces a richer scene aligned with user’s prompts. This example showcases how WonderVerse empowers users to interactively create their own customized and expandable 3D scenes.

### 9. Details on Efficient 3D Reconstruction with DUST3R

With DUST3R [43] as our 3D reconstructor, we capture 25 frames of each video and feed them to DUST3R and create point cloud with corresponding camera poses. Afterwards, we adopt ICP [3, 37] to register the sub-scene point cloud and finally output a point cloud containing the entire 3D scene.





(a) LucidDreamer



(b) Text2Room



(c) WonderWorld



(d) WonderVerse (ours)

Figure 8. Qualitative comparison with existing works for extendable 3D scene generation.





(a) LucidDreamer



(b) Text2Room



(c) WonderWorld



(d) WonderVerse (ours)

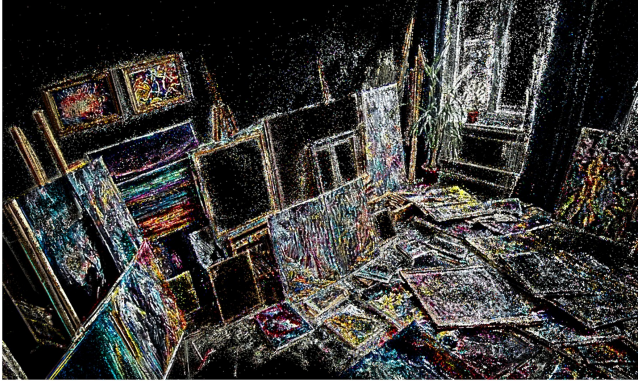
Figure 9. Qualitative comparison with existing works for extendable 3D scene generation.



**Text Input:** *An eclectic art studio filled with colorful canvases, scattered brushes, and natural light streaming through large windows.*



(a) view1



(b) view2

Figure 10. Reconstructed point clouds of our WonderVerse.

**Text Input:** *An eclectic art studio filled with colorful canvases, scattered brushes, and natural light streaming through large windows.*



Figure 11. Rendered scene of our WonderVerse.



**Text Input:** *A colorful garden filled with roses and daisies, featuring a decorative fountain reflecting the sky amidst a gentle breeze.*



(a) view1



(b) view2

Figure 12. Reconstructed point clouds of our WonderVerse.

**Text Input:** *A colorful garden filled with roses and daisies, featuring a decorative fountain reflecting the sky amidst a gentle breeze.*



Figure 13. Rendered scene of our WonderVerse.



**Text Input:** *Taj Mahal, Indian building, reflecting pool, surrounding cypress trees.*

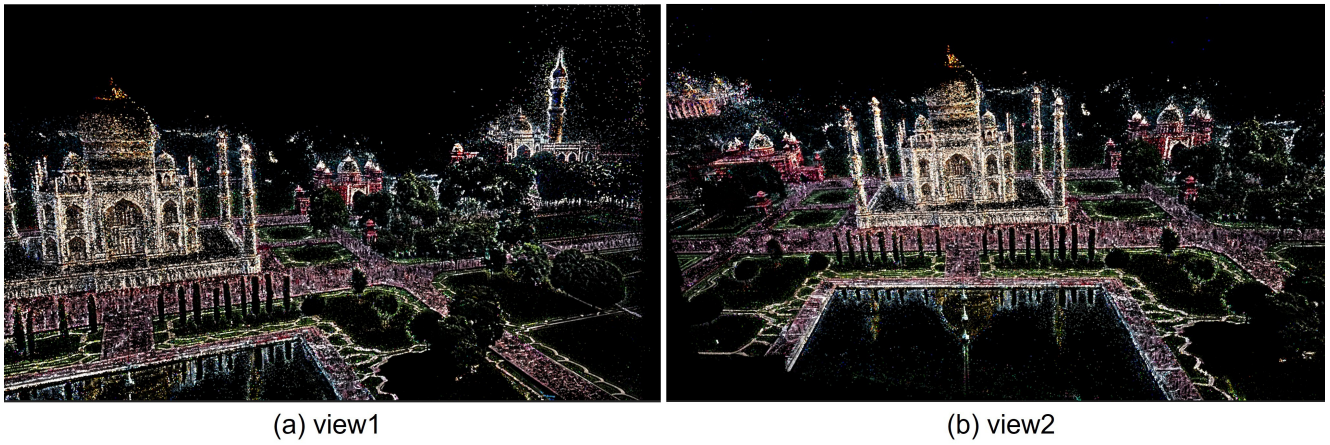
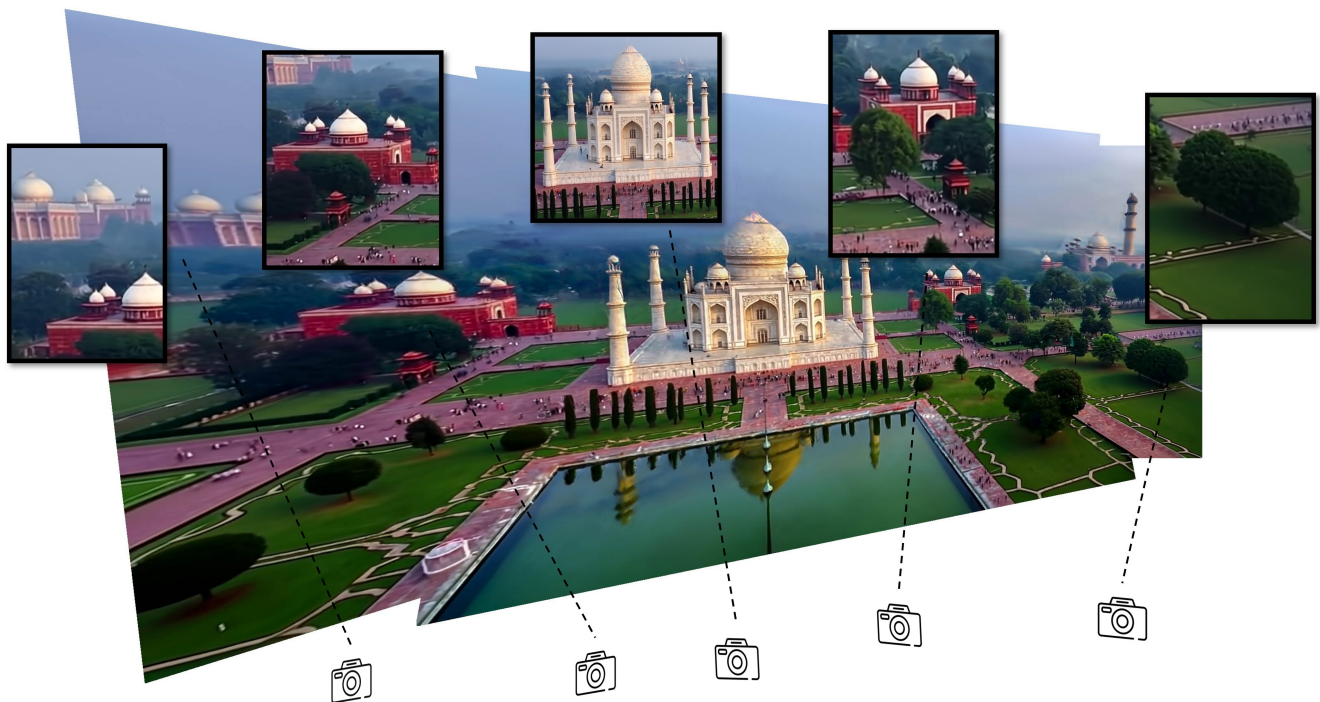


Figure 14. Reconstructed point clouds of our WonderVerse.

**Text Input:** *Taj Mahal, Indian building, reflecting pool, surrounding cypress trees.*



**Text Input:** *A futuristic Lego space station orbiting a distant planet, complete with sleek spacecraft, astronauts, control panels, and glowing stars in the background, showcasing advanced technology.*



Figure 16. Reconstructed point clouds of our WonderVerse.

**Text Input:** *A futuristic Lego space station orbiting a distant planet, complete with sleek spacecraft, astronauts, control panels, and glowing stars in the background, showcasing advanced technology.*

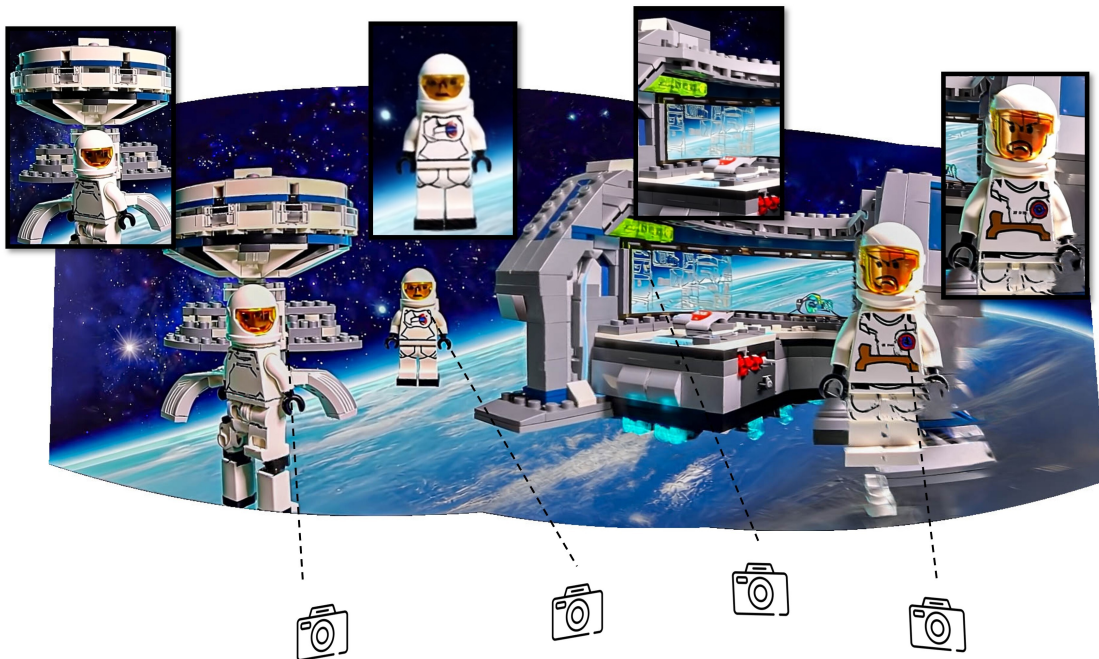
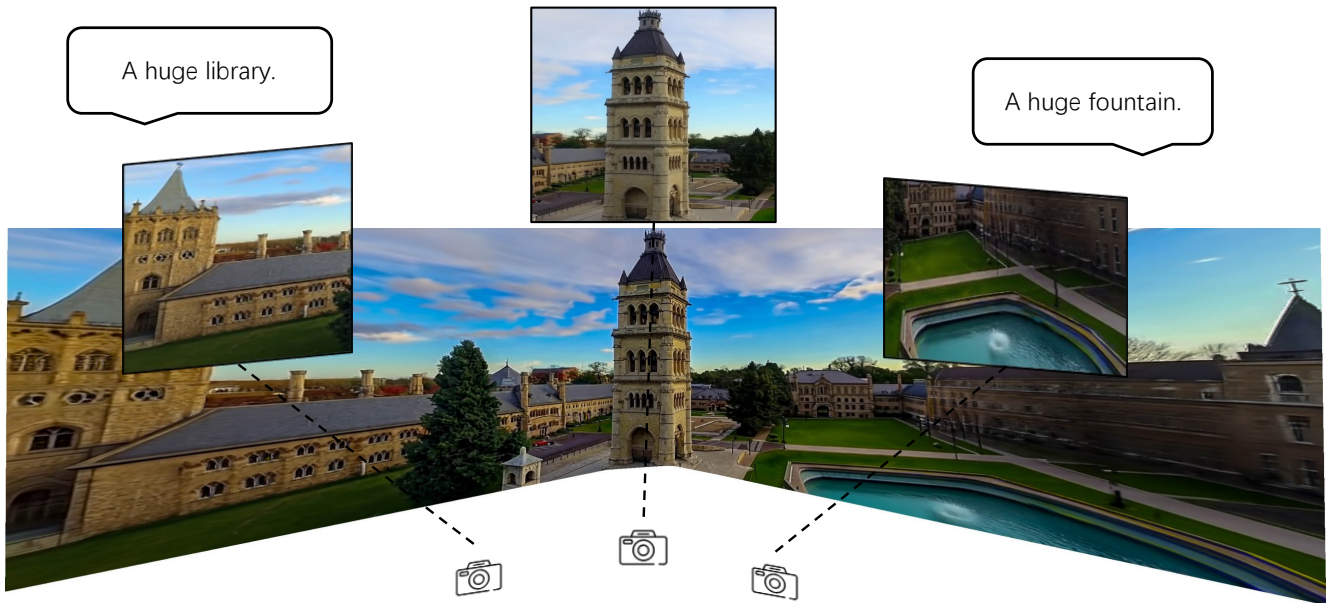
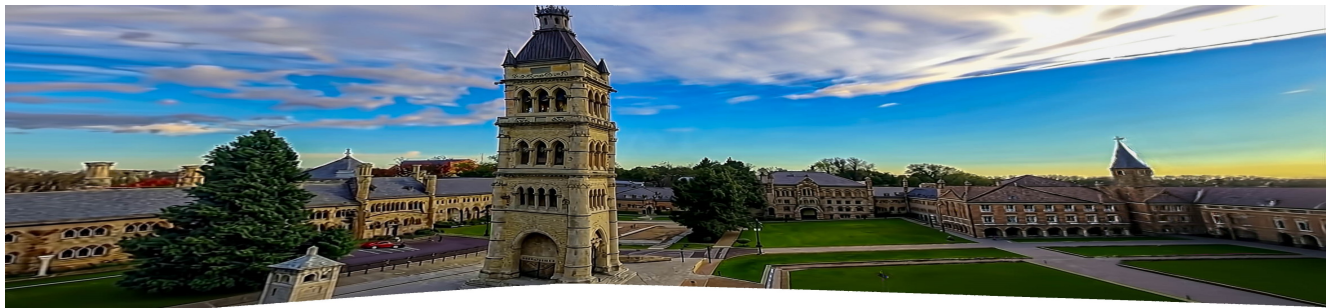


Figure 17. Rendered scene of our WonderVerse.





(a) interactive scene generation



(b) w/o interactive scene generation

Figure 18. WonderVerse’s interactive generation (a), guided by new text prompts, creates richer 3D scenes compared to non-interactive generation (b), which uses a single initial prompt for all subscenes.